



Research Article

Release of Ropinirole in Acrylate Transdermal Patches: Mutual Interactions Between Formulation Variables

Jesús Paterna-Paterna,^{1,4} Montserrat Miñarro-Carmona,¹ M^a Dolors Pujol-Dilme,² Josep Ramon Ticó-Grau,¹ and Antonio de Padua Boix-Montañés³

Received 14 December 2021; accepted 12 February 2022; published online 14 March 2022

Abstract. The aim of this study is to evaluate the interactions between formulation variables of ropinirole transdermal patches and characterize the effects of drug loading and crystallinity, degree of ionization and drug-polymer solubilization, functionalization of acrylate polymeric basis, and the addition of permeation enhancers over the release profiles. Several series of transdermal films based on carboxylic or hydroxylic acrylates (DuroTak®) and containing 1 to 10% ropinirole hydrochloride were laminated by mold-casting and evaporation. Formulations were characterized for crystallinity, drug particle size, drug assay, and residual solvents. Release profiles were obtained at different drug ionization state using paddle over disk apparatus. Mechanisms were elucidated with nonlinear data fitting of relevant release equations. Fickian and erosion processes were evaluated with the Peppas-Sahlin equation, and burst release risks were estimated as an independent term added to Higuchi kinetics. X-ray diffraction and microscopy evidenced differences in drug-polymer solubilization and density of drug crystals. Concerning drug release, area under the curve of dissolved quantities and release percentage were discriminant variables in mutual influence. Peppas-Shalin equation was the majority descriptor of release suggesting a combination of Fickian and erosion processes, revealing a decrease in the Fickian component as drug loading increased. Major burst release risks were evidenced mostly with Higuchi kinetics with vinylacetate acrylates. The carboxylic polymer without vinylacetate provided the best release extent, being more highly efficient as lower the drug loading was. Permeation enhancers with carboxylic or aliphatic radicals have, additionally, modified the release properties of ropinirole. Chemical interactions between the drug and acrylic polymers have been demonstrated. Only the effect with carboxylic polymer is pH dependent. The vinyl acetate comonomer reduces the drug release rate most effectively in formulations with low drug loads. The acrylic polymers without vinylacetate achieved the highest drug solubilization and thus the highest degree of release, providing a release of approximately 15% of the drug load.

KEY WORDS: Ropinirole; Transdermal; Acrylate-vinylacetate copolymer; Drug loading; Release.

INTRODUCTION

For decades, the pharmaceutical industry has always left the transdermal route, and in particular, transdermal patches,

in the rearguard of innovations in terms of pharmacotherapeutic treatments, partly because of the high variability in the biological and pharmacokinetic response, as well as the complexity of manufacturing these formulations, especially due to problems derived from the interaction of the drug with the polymers. In addition, it must be considered that the active ingredients must meet certain physicochemical requirements to be taken into account when studying possible formulations. Nevertheless, the use of this route confers certain biopharmaceutical advantages such as the elimination of the hepatic first-pass effect and improved adherence to the prescribed pharmacological treatment. This aspect makes it worthwhile to reconsider this route. Especially considering that certain molecules such as ropinirole have an enormous therapeutic target in a geriatric population that increases year after year with the increase in life expectancy. Optimization of drug release in transdermal formulations requires the simultaneous resolution of several challenges. In addition to

¹Unitat de Tecnologia Farmacèutica, Departament de Farmàcia i Tecnologia Farmacèutica i Físicquímica, Universitat de Barcelona, Joan XXIII, 27-31, 08028, Catalonia, 08028, Spain.

²Departament de Farmacologia, Toxicologia i Química Terapèutica, Universitat de Barcelona, Joan XXIII, 27-31, Catalonia, 08028, Spain.

³Unitat de Biofarmàcia i Farmacocinètica. Departament de Farmàcia i Tecnologia Farmacèutica i Físicquímica, Universitat de Barcelona, Joan XXIII, 27-31, Catalonia, 08028, Spain.

⁴To whom correspondence should be addressed. (e-mail: jpaterna@ub.edu)

Abbreviations: AUC, Area under the curve; EtAc, Ethyl acetate; Q24, Drug released at 24 h; ROP, Ropinirole hydrochloride; SD, Standard deviation.

acceptable skin tolerability and adequate skin adhesion, the selection of a suitable modified release polymer and the multifaceted influence of permeation enhancers are crucial parameters (1) to achieve the required release profile for an optimal skin absorption. In terms of polymer composition, acrylic copolymers have suitable solubility characteristics for a wide range of drugs and are common adhesives in many transdermal formulations. They are well tolerated on the skin and can be painlessly removed from hairy skin. Although their potential adhesiveness is lower than that of rubbers, they have largely replaced polyisobutylene because their properties remain stable over a wide temperature range, achieving very high storage stability (2). The balance between drug release rate and degree of release at laboratory scale can be achieved with preformulated grades of acrylates having different functionalizations. Drug release and, indeed, transdermal permeability of insoluble drugs depend in part on the concentration of the dissolved drug in the patches. Thus, the selection of the best conditions to provide effective drug release can be parameterized as a function of drug solubilization and followed by pharmacopoeial *in vitro* dissolution tests. Therefore, supersaturated patches with high drug ratios are often used to increase flow rates. However, sufficient and incomplete solubilization induces unpredictable burst effects and uncontrolled supersaturation compromises repeatability. In addition, oversaturation of amorphous drug can lead to physical instability, as such amorphous materials tend to crystallize in the patch (3) and drug activity and permeation decrease due to crystallization, reducing its expected skin flux due to its low dissolution rate. Although only dissolved drug molecules can permeate through the skin, some authors believe that the use of certain polymeric formulations allows for additional permeability increases over and above drug solubility that tend to be proportional to the total drug ratios (3,4). In fact, drug solubility in the polymeric matrix is a limiting factor to improve the transdermal concentration gradient. Its measurement is not easy to standardize, and it is difficult to find concrete information in the literature. As described in Sachdeva *et al.* (5), this value was calculated as the highest concentration without crystallization after stability stress. In turn, Jenquin and McGinity (6) performed measurements by differential scanning calorimetry (DSC). Some polymer manufacturers offer a user-friendly database (7) to facilitate a rough estimation of drug solubilities in their copolymers. In this aspect, relevant pharmacotechnical properties capable of modulating drug release following the degree of drug solubilization in the polymer have been evaluated. In this study, the physicochemical interactions between ropinirole hydrochloride (ROP) and different acrylates have been investigated for a set of model-formulations based on acrylic polymers with different functionalities. Ropinirole ClH (CAS: 91374-20-8) is a second-generation non-ergoline dopamine agonist that selectively activates postsynaptic dopamine receptors. The activity of ROP against Parkinson's disease is thought to be due to its stimulatory effects on central postsynaptic dopamine D2 receptors within the putamen-lock (8). It is currently used in therapeutics as a modified-release oral product and may benefit from increased bioavailability and improved patient

compliance if administered by the transdermal route. ROP is a zwitterionic molecule with acceptable biopharmaceutical properties for transdermal administration ($\log P = 3.16$, molecular weight 260.37, oral bioavailability around 50%). This drug has a remarkable water solubility and pKa values of 6.64 and 10.28 (9). The value of 10.28 is a basic pKa and corresponds to the tertiary amine, and this nitrogen is the one that will be 99% protonated in neutral conditions at skin pH. On the contrary, the value of 6.64 corresponds to an acidic pKa and specifically to the NH group of the indole ring which will not be ionized. These differences offer the possibility to study the influence of the drug ionization state over polymer–drug interactions in an acrylate-based transdermal formulation. During manufacturing of laboratory-scale laminations, interactions may occur between the drug and the coating radicals of the copolymer and with other components of the formulation, such as permeation enhancers. Interaction with permeation enhancers provides information to learn the baseline of the resultant drug release profile. These mutual interactions in the formulation environment (e.g., ionic bonding, Van der Waals forces) are prone to condition the diffusivity of the drug and have been investigated on a case-by-case basis as an essential part of the pharmaceutical development of these transdermal patches which is the main subject of this study.

MATERIAL AND METHODS

Materials

Ropinirole HCl was a gift from Disproquima (Spain). Absolute ethanol (ETH) and Ethylacetate (EtAc) were purchased from Scharlab SL (Spain). Dimethylsulfoxide (DMSO) was purchased from Guinama (Spain), Ethyl oleate (ETO), d-limonene (LIM), linalol (LIN), menthol (MNT), polyethyleneglycol 400 (PEG), and triethylcitrate (TEC) were purchased from Sigma-Aldrich (USA). Oleic acid (OLE) and propyleneglycol (PGL) were purchased from Acofarma (Spain). Three pressure sensitive adhesives with different functionalities: two acrylate-vinyl acetates with carboxylic free radicals (DuroTak 87-2051) or hydroxylic (DuroTak 87-4287) and a carboxylic acrylate (DuroTak 87-2353), named DT51, DT87, and DT53 onwards respectively, were a gift from Henkel GmbH (Germany). ROP-polymer solubilities were predicted with a commercial database (7). A 100- μm polyester foil was used as backing liner. Release liner consisted of a fluoropolymer-protected polyester (ScotchpakTM 1022) from 3M (USA).

Experimental Procedures

Ropinirole Characterization

Drug Particle size. The general method 2.9.31 of Ph. Eur. was used with a MASTERSIZER 2000 (Malvern) equipped for wet determination. Approximately 0.5 g of product was put into a beaker adding 50 ml of n-heptane. The suspension was magnetically stirred until homogenization. The addition of the sample into the unit was carried out under continuous stirring and pouring the suspension into the dispersion unit

until adequate obscuration. Samples were analyzed in triplicate and results averaged. Results were expressed as cumulative particle size distributions.

Optical Microscopy. A polarized light monocular microscope (Nikon S-P0, Japan) was used to inspect the drug powder at 200× or 400×. A minimum of ten fields were observed using a test plate of 1/4 wave to detect double refraction of crystalline findings and a micrometric scale for a rough estimation of particle size.

XRPD Analyses. Flat samples of raw material consisted of sandwiched powder between 3.6 μm thickness low absorbing polyester films. Diffractions were measured with an X'Pert PRO MPD θ/θ powder diffractometer (Malvern Panalytical, Spain) of 240 millimeters of radius, in a configuration of convergent beam with a focalizing mirror and a transmission geometry. Conditions were as follows: Cu K α radiation ($\lambda = 1.5418 \text{ \AA}$), Work power: 45 kV–40 mA, Incident beam slits defining a beam height of 0.4 mm, Incident and diffracted beam 0.02 radians Soller slits, PIXcel detector: Active length = 3.347°. Measurements consisted of 2 θ/θ scans from 2 to 60 °2 θ with a step size of 0.026 °2 θ and a measuring time of 300 s per step. The identity of individual peaks in the diffractograms was checked to match a general library of substances. The crystalline habit of the ROP in the raw material was characterized for comparison with its appearance after manufacture of the formulations.

Preparation of Formulations

Different drug percentages have been used to scrutinize possible interactions with acrylic polymers. The influence of drug loading has been checked above its maximal thermodynamic activity. Three groups of formulations were prepared as summarized in Table I:

- In a first step, each polymer (DT51, DT87, or DT53) was formulated at three content levels of ROP (1%, 5%, and 10%). The formulations were prepared under continuous stirring by dispersing the drug in ethyl acetate in closed Erlenmeyer flasks and then, adding the required amounts of DuroTak dispersion until homogeneity (30min).
- In a second stage, homologous formulations to the previous ones were prepared by dispersing the drug in EtAc, adding ETH, TEC, or DMSO (5% final concentrations before drying) and, finally, the required additions of the carboxylic acrylate DT53.
- In a third stage, a set of formulations with 5% ROP in DT53 was similarly prepared with a series of permeation enhancer candidates widely described in the literature (OLE, ETO, PGL, PEG, LIM, LIN, MNT). Each substance was added at 5% at the end of the mixing preparation.

Laboratory-scale laminar patches were prepared by mixing the components with EtAc under magnetic stirring

in closed Erlenmeyer flasks. The calculated amount of ROP was added to the mixture to reach 1, 5, or 10% ROP by weight of dry polymer and stirred for 5 min until complete dispersion in the polymer mixture. Laminations were prepared pouring the dispersion over the release liner mounted in a mold to obtain a uniform plate. After 10 min at room temperature, the plate was then heated inside the mold to slowly evaporate volatile contents over 60 min with progressive thermoelectric heating up to 50 °C (1,10,11). After drying, gravimetric analysis and gas chromatography confirmed the absence of residual solvent and thus the cure of the formulation. The adhesive side of the lamination was then protected with a 3M Scotchpak™ 9732 polyester protective film and die-cut into circular specimens. The final thickness was determined with a digital micrometer, obtaining mean thickness values of 146 μm with a coefficient of variation of 10.46%. The samples were stored hermetically until the investigation of the ROP release. The drug content (dose) for each batch after drying process was estimated w/w from the composition of the dispersion and the amount of dispersion poured over the liner.

Evaluation of Formulations

Residual Solvent. Only EtAc has been used in the formulation aiding to acrylics dissolution and fluency tuning to facilitate the homogeneous dispersion of the components. ICH specification (12) for EtAc as a residual solvent in final products (<5000 ppm/24h) has been considered as an indicator to check the endpoint of the drying step. GC gas chromatograph (ThermoFisher Scientific) consisted of an automatic injector TRIPLUS module Head Space-Trace coupled to DSQII mass spectrometer. Analysis was performed with a capillary column: Zebtron®ZB-624plus (Phenomenex, Spain) at an injector temperature of 220°C using helium as a carrier gas with a flow rate of 1.8 mL/min. The ionization mode was by electronic impact.

Optical Microscopy. Samples of all the laminate formulations were observed under Microscope (Nikon S-P0, Japan) at 200× or 400×, as previously described, using a micrometric scale. Representative photographs were recorded.

X-Ray Powder Dispersion. X-ray crystallographic analysis was performed to check the presence of crystals in the formulations. Samples were prepared as described above. Figure 1 shows the comparative diffractograms of each sample (see legend). Peaks assigned to the polyester-support layer and ROP (at 2 θ 7.4 and 11.4) are identified in all samples. Some additional peaks in the diffractograms of the dispersions could be assigned to paraffin oil and calcium carbonate at 2 θ 21.5 and 29.5, probably originating from the release liner and DuroTak respectively. X-ray intensity data were measured on a Siemens P4 diffractometer using MoK α radiation ($\lambda = 0.71073 \text{ \AA}$) and the 2 θ/θ scan technique. Semiquantitative proportions of crystals in each formulation were estimated and reported.

ROP Tautomerism in Analytical Samples. Due to its structural characteristics (see Fig. 2), ROP can

Table I. (continued)

Phase of the study	STAGE 3
5%	5%
5%	5%
5%	5%
5%	5%

tautomerize in aqueous solution. In fact, during the set-up of the analytical method, a slightly yellowish coloration of samples was observed after few days which could potentially affect the spectrophotometric readings. Thus, the tautomerism equilibrium in our experimental conditions was checked with a proton-NMR to determine the differences in the proton spectra of each of the three possible tautomer's (see Fig. 2). Subsequently, an assay was performed with ¹H-NMR and ¹³C-NMR in ROP aqueous solutions at 72h. Results matched with those obtained from the experimental spectra confirm that the majority tautomer corresponds to form A and the minor corresponds to B tautomeric form, while tautomer C is not detected (see Fig. 3). The acidity of the medium (pH 6) would facilitate the formation of tautomer B and a mixture of tautomers is detected, while in neutral solutions only the presence of tautomer A is observed. Tautomer B presents a conjugation between the two aromatic rings not seen with tautomer A this would be the cause of the yellow color. Finally, a confirmatory test was performed by preparing three ROP calibration lines that were measured at time zero and 3 days later to check for possible variations between the two times. A one-way ANOVA of the slopes with respect to time was performed (alpha=0.05) discarding differences. Consequently, the tautomerism of ROP under our experimental conditions does not disturb its spectrophotometric determination.

Drug Release. Dissolution test following pharmacopoeial apparatus V (Erweka DT 80, Gomensoro, Spain) was used with 500 mL pH 6.00 or pH 10.00 glycine buffer solutions (13) satisfying sink conditions. Laminar samples from the stage 1 formulations were tested in quadruplicate for 36 h. Twelve 5-mL samples were taken at 0h, 0.5h, 1h, 2h, 4h, 8h, 12h, 18h, 24h, 30h, 34h, and 36h with immediate buffer replenishment. Drug concentrations were estimated by UV spectrophotometry (Cary 60 UV-VIS, Agilent, USA) with linearity demonstrated at the maximum absorbance of ROP at 250 nm (14). Samples of stages 2 and 3 formulations were similarly tested in quadruplicate at pH 6.00 for 24 h.

Calculation of Descriptive and Explicative Release Parameters. Individual release profiles were plotted prior to parameter calculation. All individual curves were described with amodelistic parameters, as follows, for further statistical comparison. Dissolved amounts at 24h (Q24), released drug fraction (F) and area under the curve of released quantities (AUCq) were calculated for each replicate with an Excel Worksheet. The following explicative equations (in respective order) of time-dependent released drug fractions (F) were fitted by non-linear regression using DDSolver (15): Higuchi (Eq. 1), Higuchi F₀ (Eq. 2), Peppas-Sahlin 0.5 (Eq. 3), and first order-F_{max} (Eq. 4) (16–19):

$$F = k_H \cdot \sqrt{t} \tag{1}$$

where k_H is the Higuchi release constant.

$$F = F_0 + k_H \cdot \sqrt{t} \tag{2}$$

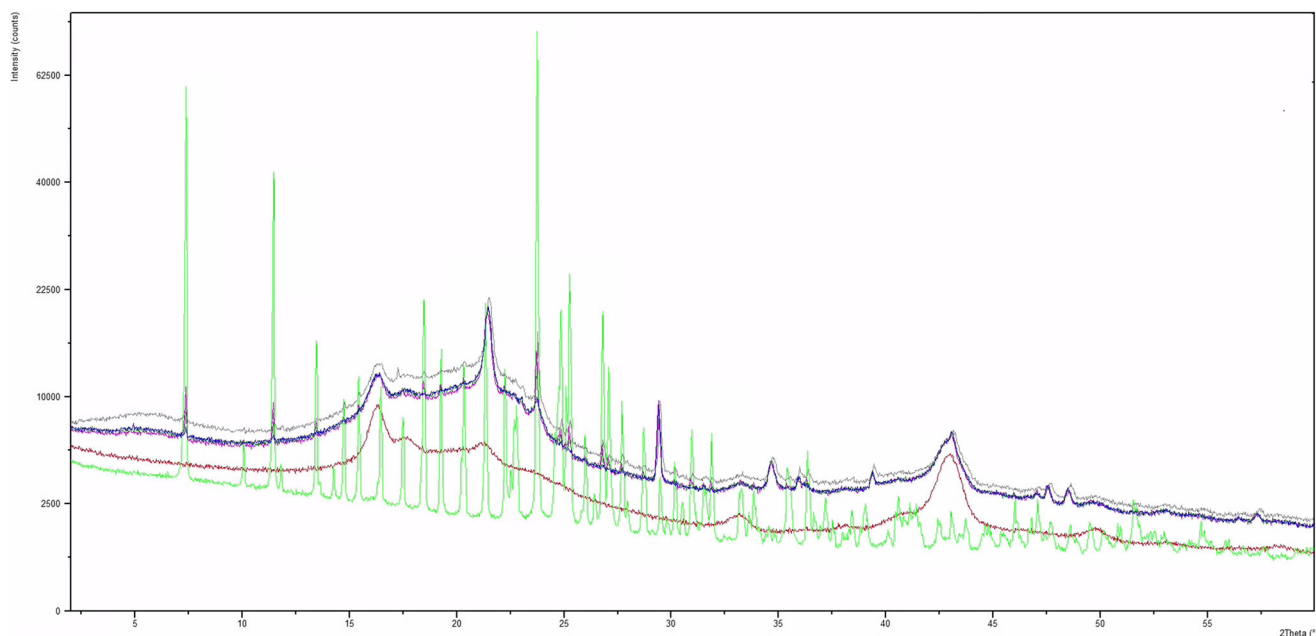


Fig. 1 XRPD peaks of the different formulations compared to the reference sample without ROP. Polyester material (red), reference ROP (light green), 10% undissolved ROP dispersion (pink), 5% undissolved ROP dispersion (dark green), 5% ROP dispersion dissolved in ethanol (grey), and 1% undissolved ROP dispersion (blue)

where k_H is the Higuchi constant and F_0 is the initial drug fraction in solution generated by a burst release.

$$F = k_1 \cdot \sqrt{t} + k_2 \cdot t \quad (3)$$

where k_1 is the constant about the relative contribution of drug diffusion to drug release and k_2 is the descriptive constant of the time-dependent polymer relaxation. The exponents were the proper values for laminar formulations.

$$F = F_{\max} \cdot 1 - e^{-k_1 \cdot t} \quad (4)$$

where F_{\max} is the maximum amount of released drug at infinite time and k_1 is the first-order constant.

Additionally, a non-explicative biexponential equation was also used as a descriptive tool if none of the previous equations were successful:

$$F = 100 \cdot \frac{e^{(\alpha + \beta \cdot \log_t)}}{1 + e^{(\alpha + \beta \cdot \log_t)}} \quad (5)$$

where α is the scale factor and β is the shape factor in the logistic distribution.

Model Selection and Parameters Comparison. Amodelistic parameters were compared by curves inspection and a one-factor ANOVA (SPSS v.26) of AUC_q and Q24 between comparable series (stage 1) or between the basal formulation and each enhancer (stages 2 and 3).

Selection of the best model for each case was based on the observation of graphs, best observed-predicted adjusted determination coefficient (Rsqr max), minimum Akaike information criterion (AICmin), and subrogated model selection criterion (MSCmin) given by DDSolver software. The major best-fit for each set of replicates was reported. In cases where Peppas-Sahlin (Eq. 3) was the best descriptive function, Eq. (6) (18) was used to describe the progressive reduction of the contribution of the Fickian component (15) in the whole release:

$$F = 1 / \left(1 + \left(\frac{k^2}{k^1} \right) * \sqrt{t} \right) \quad (6)$$

Then, the contribution of the erosive component in the resulting release profile was assessed by graphical comparison of the corresponding plots of the mean values of each set of replicates.

RESULTS AND DISCUSSION

Ropinirole Characterization

Particle Size

The most frequent particle size of the ROP raw material was 8.70 μm following a distribution shown in Fig. 4 where 97.07% of the particles were smaller than 98.00 μm . Micrometric measurement by optical microscopy yielded results of the same order.

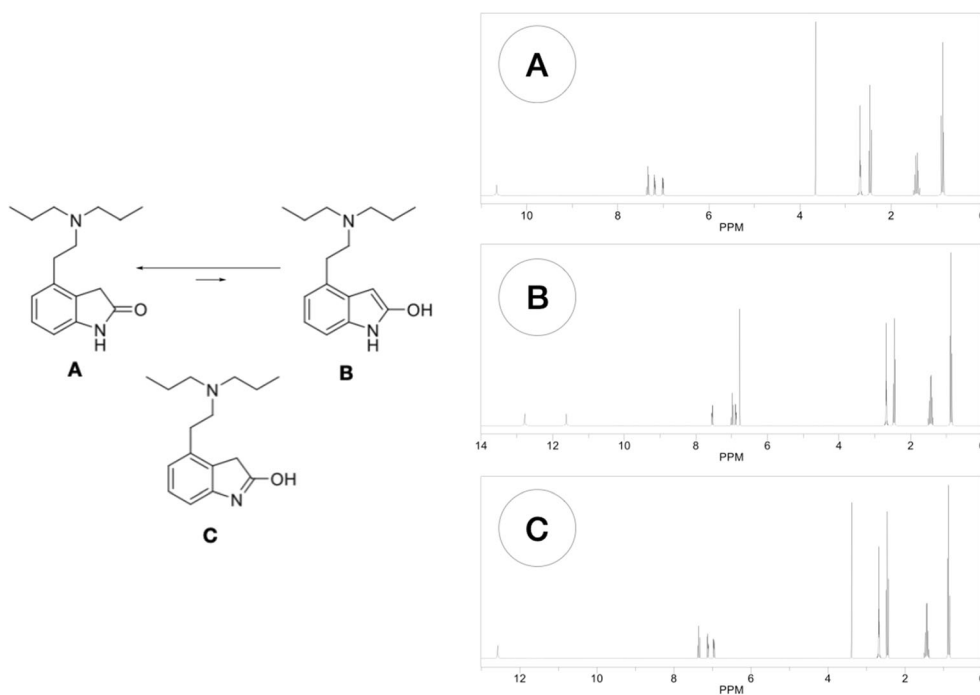


Fig. 2 Transition of the different ROP tautomers and theoretical ¹H-NMR spectrum of tautomers (A, B, and C)

X-Ray PD Analysis

Crystalline structure of ropinirole hydrochloride drug powder corresponds to the triclinic habit of Cambridge Structural Database:

$$a = 7.5388(11)$$

$$\text{\AA}, b = 8.9545(13) \text{\AA}, c = 12.1647(18) \text{\AA},$$

$$\text{alpha} = 80.005(2)^\circ, \text{beta} = 85.968(2)^\circ, \text{gamma} = 83.504(2)^\circ$$

These crystals are associated with a singonic ellipsoid with three unequal axes. It means that crystals have no

orthogonal angles and axes are unequal (20). In other words, crystals are prismatic oblicuous and asymmetric.

Evaluation of Formulations

Residual Solvents

A representative GC-MS chromatogram is shown in Fig. 5, and Fig. 6 shows the individual EtAc levels in the different batches. All values are below the ICH specifications, which confirm complete drying and ensure that the procedure is reproducible. Also, it has been observed that the higher the drug loading, the higher the amount of residual solvent, regardless of the polymer used.

Crystallinity by X-Ray PD

The crystalline habits in the different dispersions and the

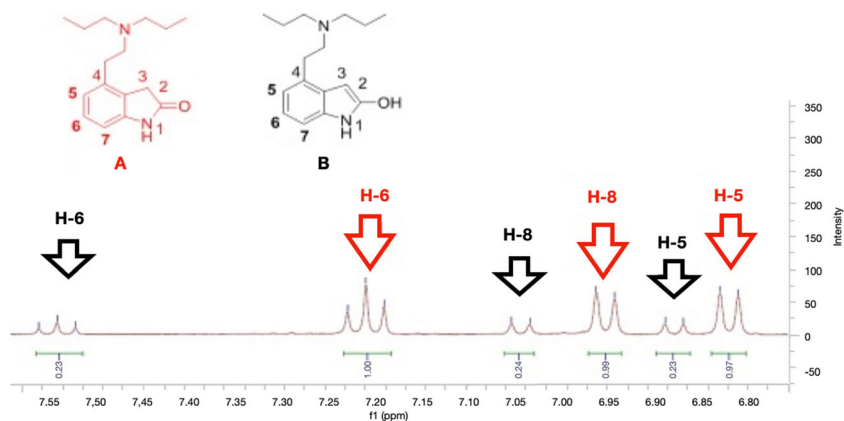


Fig. 3 Aromatic zone of the experimental ¹H-NMR of the ROP tautomer A (majority, red color) and B (minoritarian, black color)

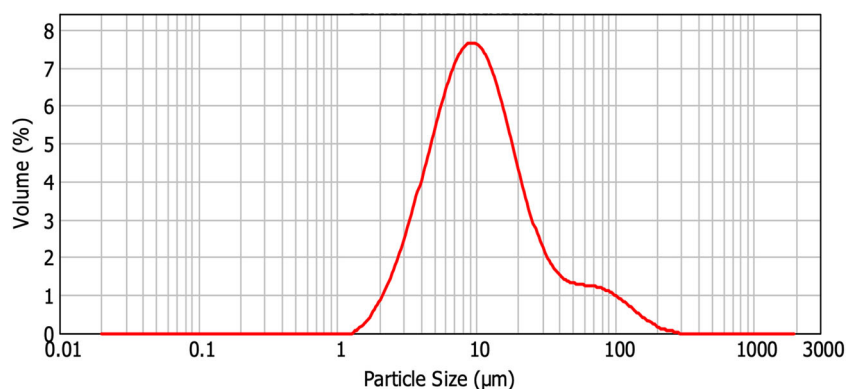


Fig. 4 Logarithmic scale plot of particle size dispersion

precipitated drug were also identified as well as the powdered drug. This fact confirms that intermediate solubilization was not achieved.

Drug–Polymer Solubilization

All solubilities of ROP in polymers predicted with the database were lower than 1% ($^{w/w}$) and in the following rank: DT51 \geq DT53 > DT87. Values predicted for both carboxylic acrylates (DT51 and DT53) were similar and higher than for the hydroxylic one (DT87). Thus principle, all formulations were prepared above their respective solubilities predicted. Otherwise, after curing, formulations were inspected with polarized light optical microscopy. Crystalline particles below 35 μm were observed (DT51 and DT87). No differences in the mean number of insoluble particles per field seemed to be detected between both polymers. In case of DT53, a continuous conoscopic refringence was observed. Illustrative images are depicted in Fig. 7 (17). Integration of the major peaks of the XRPD diffractograms of the dispersions reveals a crystalline phase in the following semi-quantitative proportions: 10% dispersion

(approx. 8.60%), 5% dispersion (3.80%), and 1% dispersion (1.40%). The origin ordinate of 0.298% could be taken as a rough estimate of the saturation level of the drug in the DT53 polymer. As for the 5% ROP formulation with ETH, 4.7% was estimated, suggesting that no additional supersaturation was achieved with the initial solubilization with ethanol and subsequent evaporative precipitation. This formulation became transparent during dispersion until mold casting. After lamination, the slide appeared homogeneously refractive at 200 \times (Fig. 8). Observations at 400 \times revealed the existence of a homogeneous dispersion of crystals below 10 μm . Formulation with TEC appeared as a solid non-refringent image. The formulation with DMSO showed a low-size population of crystals identified also below 10 μm . Both dispersions remained translucent without achieving transparency at any time (see Fig. 9 A and B respectively). All formulations containing enhancer candidates (stage 3) showed a typical refringence as observed in stage 1 with the same polymer DT53. Figure 9 shows the photographs of the formulation with OLE and ETO (c and d respectively), which have given the highest and the lowest release as described ahead in Table V.

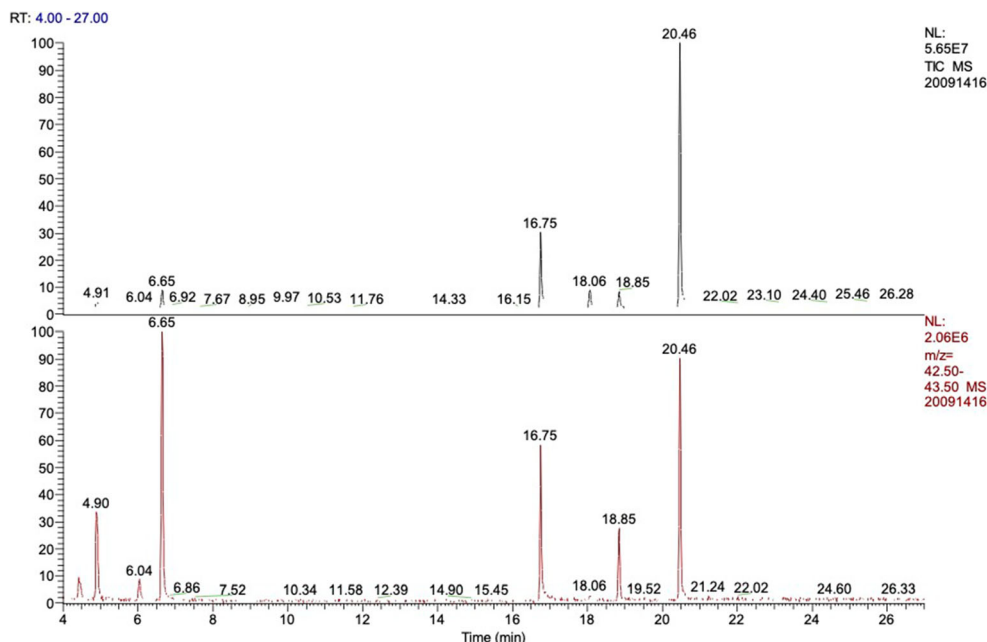


Fig. 5 Representative GC-MS chromatogram showing that the EtAc peak appears at 6 min

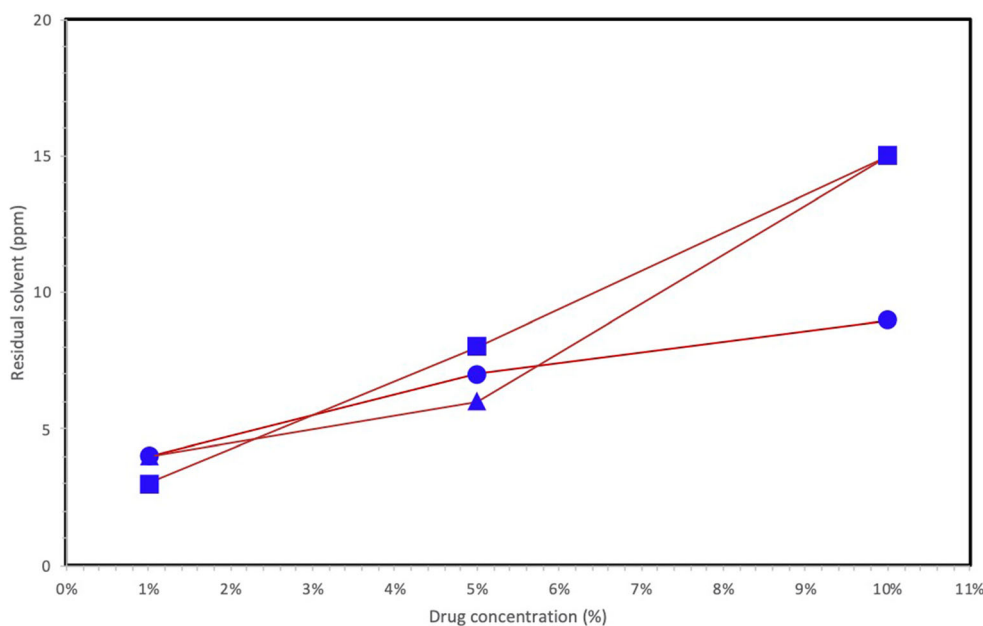


Fig. 6 Residual solvent of each formulation

Drug Release

Results grouped by experimental sets ($n = 4$ replicates). A representative plot of the remarkable differences is reported in Fig. 10. *Release Parameters Concerning Polymer Selection (Stage 1)*. Mean and SD results of AUC_q (until 36h) and Q₂₄ for each set of replicates are summarized in Table II. The highest release values were achieved with DT53. Statistical significances of the ANOVA comparisons as a function of pH or drug loading are summarized in Tables II and III. Results point to the effects of pH over both carboxylic acrylates (DT51 and DT53) accounting for higher values of AUC_q and Q₂₄ at pH 10.00 than in pH 6.00. This effect was more pronounced in absence of vinylacetate (VA). Statistical significance (Table III) is achieved in all cases concerning DT53 (carboxylic acrylate) and only in DT51 high-load level. Conversely, this effect does not occur with the hydroxylic acrylate (DT87). Concerning model fitting, MSC results were fully concordant with AIC comparisons without any additional descriptive information so, being parsimonious, all the model selections were primarily based on AIC as summarized in Table IV. This discrimination analysis points to Peppas-Sahlin (1989) (18) (Eq. 3) as the best descriptive

equation for the acrylate DT53 profiles except for the lowest concentration at pH 6.0. Moreover, the acrylate-vinylacetate copolymers (DT51 and DT87) exhibited a lower release extent than DT53, and Higuchi- F_0 was more descriptive than Peppas-Sahlin when notorious burst effects were present (21). In fact, burst release was higher with DT51, the most retentive of the three polymers. Based on the parameters of Peppas-Sahlin, the main effect over the Fickian and non-Fickian release was observed with Eq. (6) at the different drug load levels (see Fig. 11). No differences were observed between pH values for the homologous formulation. As seen on Fig. 12, the erosion predicted for the matrices with 10% ROP was higher than the corresponding values achieved for 1% ROP.

Release Parameters Concerning the Effect of Permeation Enhancers (Stage 2 Formulations). Results of AUC_q (until 24h) and Q₂₄ for each enhancer candidate are summarized in Table V (mean and SD). ANOVA demonstrated maximal statistical significance of differences between the basal and OLE. Concerning AUC_q, differences were demonstrated for all the Q₂₄ values except for MNT. All release profiles were described with Peppas-Sahlin equation except for the OLE

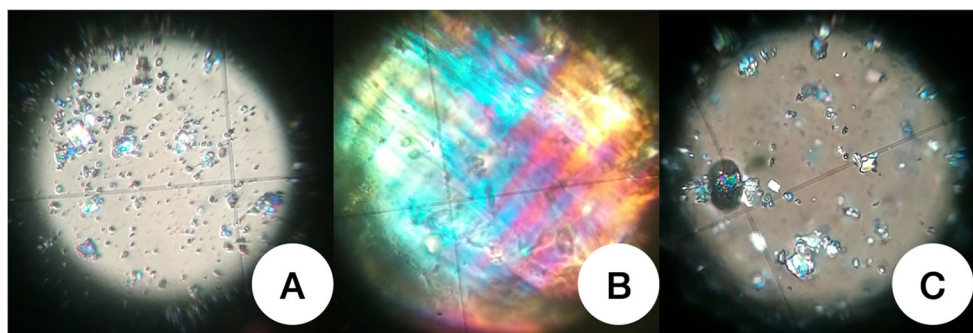


Fig. 7 Optical microscopy 200 \times with polarized light of laminates of 5% ROP dispersions in DT51 (A), DT53 (B), and DT87 (C)

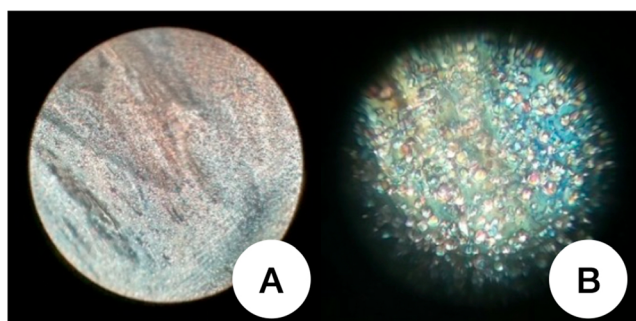


Fig. 8 Optical microscopy with polarized light of laminates of 5% ROP with 5%ETH in DT53 at 200× (A) and 400× (B)

formulation where the logistic equation resulted to be more suitable in terms of minimum AIC and plausibility of predicted profiles. A comparative plot of mean ROP profiles in pH 6 with the laminates having aliphatic enhancers appears in Fig. 13, being higher for the carboxylic (oleic) and lower (oleate) for the carboxylate. It demonstrates the relevant influence of the carboxylic radicals at neutral pH.

Degree of Dispersion

Microscopic inspection confirmed the presence of crystals in dispersions based on DT51 and DT87 acrylate-vinylacetate copolymers. The size of the crystals is in the same range as the observed particle size of the ROP powder suggesting no crystal growth observed. It confirms that no intermediate solubilization in ethyl acetate has occurred during dispersion preparation. In the case of the acrylic polymer (DT53), a pseudo-dissolution of the drug in the polymer matrix suggests a significantly higher solubilization

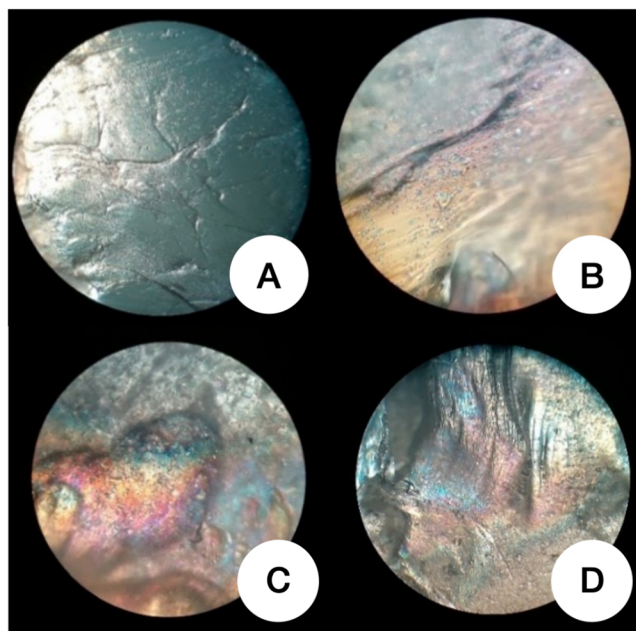


Fig. 9 Optical microscopy 200× with polarized light of laminates of 5% ROP in DT53 having 5% TEC (A), 5% DMSO (B), 5% OLE (C), and 5% ETO (D)

than with the DT51 copolymer, although the numerical predictions of the solubilities were similar. This database prediction is poorly discriminating because it only requests the logP and water solubility values of the drug and has not discriminated the effect of VA. With respect to stage 2 formulations, it was observed that 5% ethanol achieved solubilization of ROP, but reverse insolubilization appeared when the solvent was removed during evaporation. This insolubilization was subsequently confirmed by optical microscopy (5). In fact, a population of uniformly sized crystals with an almost spherical growth habit was observed instead of the original heterogeneity of the raw material observed with DT51 and DT87. TEC can act as a plasticizer by reducing the glass transition temperature of acrylates. This formulation can modify the physical state of the acrylic dispersion. Microscopic observations are inconclusive because no crystals are observed and no solubilization has been observed during the formulation process. As for DMSO (22), crystals of the drug of the same particle size as the original were observed, suggesting its non-solubilization.

Effect of Drug Loading and pH-Dependent Interaction

Regarding drug loading, all formulations are oversaturated (7). Statistical differences between the released fractions are found in practically all cases (see Table VI). Differences in the extent of release, expressed as AUC_q, are greater the higher the drug loading becomes, although they are not linearly proportional to the ROP concentrations in the case of the more retentive formulations. In addition, Q24 percentages are indicative of formulation efficacy, and the value at 24 h (66% of the experiment) is more discriminant of the shape of the curve than the value at the last time (36 h). As an example, the Q24 values of the 1% formulations are higher than the respective values at 10%, and the absolute released amounts (although statistically different) tend to be closer to each other than at first appearance. Therefore, drug utilization (efficiency) with retentive polymers (DT87 and DT 51) is better at low drug loading levels. However, drug release from DT53 is practically proportional to its drug loading, and, therefore, efficiency is practically similar for all three loadings, with DT53 achieving the highest extent and efficiency (14.97% when considered as a whole). As for the effect of pH, the interaction of the tertiary amine of ROP with carboxylic polymers (DT51 and DT53) has been detected. The results at pH6 are due to the presence of positively charged ROP, whereas at basic pH, it is negatively charged. This effect was clearly more noticeable with DT53, free of VA. It can be assumed that the retention of ROP by these polymers is the result of the combination of both the ionic interaction (carboxylic-amine), which depends on pH, and a polarity component that implies a higher retention of the drug in absolute terms for the more lipophilic the polymer with VA (DT51 or DT87) given the insolubility of this comonomer. The release from DT87, a hydroxyl-only copolymer and therefore not pH-sensitive, was statistically different from DT53 but not from DT51, probably due to its similar VA content. Overall, the differences in drug release depend more on the presence and/or absence of VA, an insoluble comonomer, than on the interaction with carboxylic or hydroxyl residues. These observations are related to the

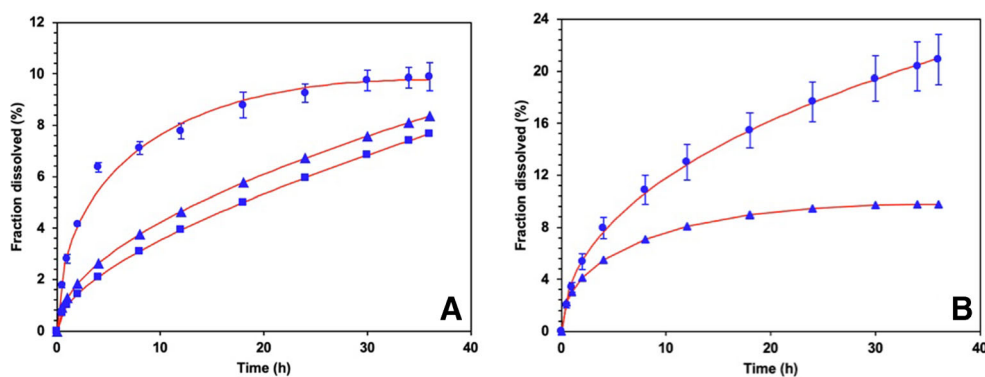


Fig. 10 Experimental release points (blue) and predicted profiles with Peppas-Sahlin equation (red lines) of ROP formulated in DT53. **A** Mean profiles at pH 6 from 10% (circle), 5% (triangle), and 1% (square) formulations; **B** Mean profiles of 10% formulation at pH 6 (triangle) and pH 10 (circle). Standard deviations are indicated for the fastest profiles

Table II Amodelistic release parameters, AUC (mg*h) and Q24 (mg) in the different conditions

Polymer	Drug concentration	pH	AUCq(36h)	SD _{AUC}	Q24	SD _{Q24}
DT51	1%	6	4010.31	461.97	7.25%	0.65
	5%	6	4257.70	2263.93	1.37%	0.70
	10%	6	6519.53	1202.29	0.92%	0.24
DT51	1%	10	4250.77	1334.82	5.66%	1.35
	5%	10	5096.31	998.21	1.88%	0.43
	10%	10	9797.59	1113.25	1.67%	0.28
DT53	1%	6	2465.69	240.98	6.08%	0.92
	5%	6	13,838.46	1100.00	6.11%	0.27
	10%	6	45,965.68	2346.86	9.26%	0.35
DT53	1%	10	6439.40	1672.07	14.45%	2.81
	5%	10	26,764.40	1395.65	12.79%	0.85
	10%	10	79,751.50	3268.24	17.66%	1.55
DT87	1%	6	4470.79	1718.34	9.27%	2.76
	5%	6	13,205.45	646.84	5.36%	0.64
	10%	6	15,313.37	4873.60	3.83%	1.65
DT87	1%	10	4151.08	835.52	8.63%	1.06
	5%	10	12,706.81	1134.98	5.64%	1.49
	10%	10	13,022.45	3014.94	2.75%	0.80

Table III Effects of pH on release profiles considering amodelistic parameters. Statistical probabilities (significances in bold)

Polymer	AUCq (mg/h)			Q24 (mg)		
	1%	5%	10%	1%	5%	10%
DT51	7.45E-01	5.23E-01	7.11E-03	1.04E-01	2.63E-01	6.79E-03
DT53	3.31E-03	6.62E-06	2.85E-06	1.31E-03	5.51E-06	4.26E-05
DT87	7.49E-01	4.74E-01	4.54E-01	6.80E-01	7.39E-01	2.84E-01

degree of dispersion observed with optical microscopy. It is confirmed that the degree of release is facilitated by using DT53, the polymer with the highest degree of solubilization. The effects of pH and drug loading are only revealed with the polymer without VA (DT53), whose hydrophilicity facilitates the entry of water for dissolution. In this sense, the addition of minor components in the formulation to modify the

ambient pH could be used for a fine optimization of the drug release profile if the polymer is suitable.

Descriptive Equations of the Release Mechanism

Released Eqs. (1) to (4) have been selected to analyze the influence of polymer erosion and/or the relevance of the

Table IV Best descriptive equations for each set of replicates based on AIC values (H: Higuchi, HF₀: Higuchi with F₀, PS: Peppas–Sahlin 0.5)

Polymer	pH6			pH10		
	1%	5%	10%	1%	5%	10%
DT51	HF ₀	PS	HF ₀	HF ₀	PS	PS
DT53	HF ₀	PS	PS	PS	PS	PS
DT87	PS	H	PS	PS	H	PS

non-occluded drug (burst effect) on the drug release profiles. Regarding the bursting effects, the drug loading was well above the solubilization capacity of the polymer, and this effect in the 10% formulations is higher than in the respective 1% formulations, as observed in Fig. 10. Considering the microscopic observations discussed above, after bursting, the release kinetics with the formulations containing crystals (DT51 and DT87) may not follow a first order release, but a pseudo-square root kinetics, indicative of solubilization of the crystals prior to its release. This equation tends to be more descriptive for the more retentive copolymers, probably with lower solubilities than DT53. All drug release profiles from DT53, the least retentive copolymer, follow the Peppas–Sahlin equation, a combination of burst-erosion (oversaturated drug proportion) and diffusion (dissolved drug). In addition to these solubilization properties of the polymer, the interaction of -COOH functional groups with amine-containing compounds through hydrogen bonding (23) has influenced the rate and extent of *in vitro* release of ROP, but not the kinetic mechanism.

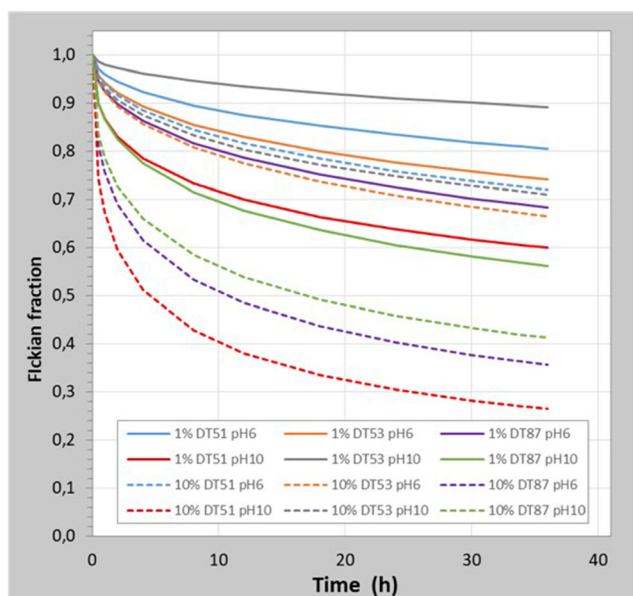


Fig. 11 Loss of Fickian diffusion along the experimental time for all the formulations at the minimum and the maximum drug load. Continuous lines: 1% load, dotted lines: 10% load

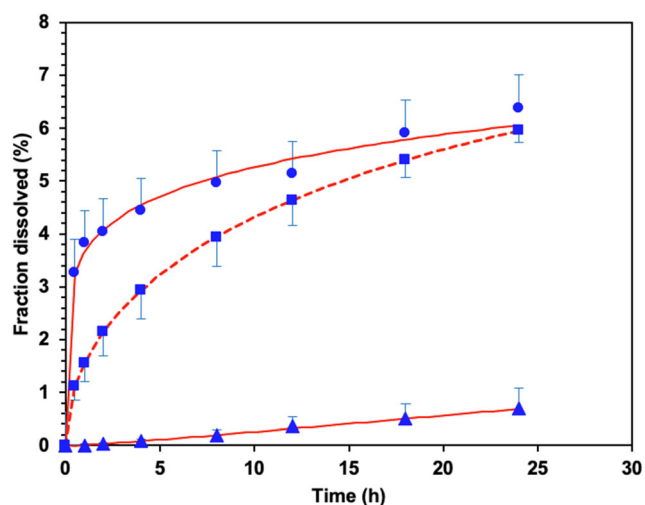


Fig. 12 Mean ropinirole release profiles of OLE (circles), ETO (triangles), and basal (squares, dotted line) formulations

Influence of the Permeation Enhancers Over Ropinirole Release Profile

After having selected DT53 as the best suitable polymer, the interaction of ROP with carboxylic radicals at skin pH6 in the presence of permeation enhancers has been investigated. Overall, the fit of the release equations to the experimental results has confirmed the previous hypothesis on the expected diffusion-erosion kinetic mechanism. Only the fastest release profile is not well described with Peppas–Sahlin. In this case, an empirical equation is more descriptive. As a representative example, Fig. 13 shows a visual comparison between the two settings suggesting the inability of the diffusion-erosion model. The described physicochemical properties of ROP and the conditions of the experimental study have been demonstrated as essentials to modulate the release profile. In fact, the inclusion of an acidic permeation enhancer (oleic acid) has excessively increased the extent of ROP release, probably by an additional bursting effect due to the uncoupling of the drug from the polymer. On the other hand, a reverse effect has been found in the presence of a homologous aliphatic cosolvent (ethyl oleate) which hinders the release of the drug into the aqueous medium. The greatest increase of drug release at this pH has been found with oleic

Table V Amodelistic release parameters (mean and SD, n=4) for the 5% ROP laminates in DT53 containing 5% enhancers (aliphatics, glycols or terpenes). Values statistically different from the basal formulation are in bold

Substance	AUC _{q(24h)} mg/h	SD _{AUC} mg/h	Q24 mg	SD _{Q24} mg
none	7426.29	964.94	443.38	30.50
OLE	10,941.07	423.78	546.70	23.38
ETO	549.15	559.94	44.39	41.46
PGL	2520.72	509.47	131.57	25.53
PEG	6118.16	396.35	302.50	28.11
LIM	2282.63	340.95	151.47	32.48
LIN	2917.37	578.17	204.93	35.39
MNT	6381.92	2280.10	338.45	102.60

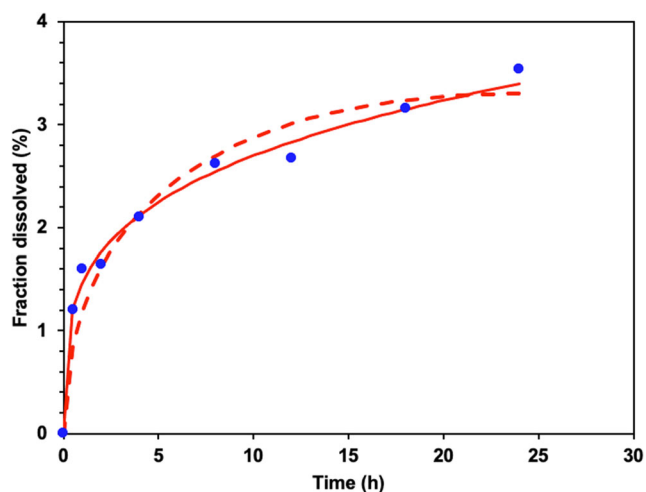


Fig. 13 Individual data fitting of a single replicate-example of OLE (circles) using Peppas-Sahlin equation (continuous line) and the logistic equation (dotted line)

acid, a fatty acid, resulting in an increase in the extent of release at early times. It can be hypothesized that the carboxyl radical of this non-polymeric substance competes for drug binding with the carboxyl residues of DT53, decreasing the ionic interaction of the ROP with the acrylic matrix. This increases the mobility of the drug and its degree of release. ETO, which is an ethyl ester of fatty acids, usually favors the solubilization of lipophilic drugs. This cosolvent probably hinders the release of ROP into the aqueous medium of the dissolution vessel. Consequently, the removal of the drug from the acrylic matrix has been further reduced to extremely low levels by sequestration, as shown by the lowest AUC_q(24h) values found. As for enhancers with solubilization properties, PGL or PEG, which are hydrophilic polyols, relevant effects on Q24 but not on the extent of release have been detected. In relation to sesquiterpenes, the addition of LIM or LIN (liquids) has reduced the levels of Q24 and AUC_q(24h) but not with MNT (solid) which is a secondary alcohol. The use of ETH has increased the presence of crystals by recrystallization, decreasing the release profile of the ROP, being significantly lower when the ROP is in crystalline form since, according to Williams *et al.*, solid dispersions containing the drug in amorphous form generally show much faster dissolution rates than formulations containing the crystalline drug, leading to significant improvements in drug absorption (24).

Table VI Effects of drug loading on release profiles considering amodelistic parameters. Statistical probabilities (significances in bold)

Polymer	AUC _q (mg/h)		Q24 (mg)	
	pH6	pH10	pH6	pH10
DT51	8.03E-02	1.65E-04	1.10E-04	1.27E-04
DT53	4.29E-11	1.66E-11	5.78E-05	1.67E-02
DT87	1.49E-03	1.48E-04	7.63E-03	1.83E-04

CONCLUSIONS

During the development of a transdermal formulation of ROP, the presence of an interaction between the drug and acrylic polymers is confirmed. The presence of vinyl acetate comonomer reduces the drug release rate, identifying these polymers as “retentive”. Similar drug release levels are similar regardless of drug loading and functionalization. The greatest efficacy with these formulations is achieved at low drug loading. Carboxylic polymers provide pH-dependent release properties, whereas hydroxyl polymers do not. Acrylic polymers without vinylacetate achieved the highest drug solubilization and thus the highest degree of release, providing release of approximately 15% of the drug load. The influence of other formulation components, such as permeation enhancers, on the release profile of ROP when carboxy-amine binding could occur and by competitively hindering the aqueous solubilization of ROP has also been demonstrated.

ACKNOWLEDGEMENTS

Authors wish to thank Henkel Corp. for supplying DuroTak samples, the “Departament de Productes Naturals, Biologia Vegetal i Edafologia” of the Faculty of Pharmacy at the University of Barcelona for its assistance in optical microscopy, SCT at Universitat de Barcelona for its assistance in XRPD and residual solvent analysis, and Mrs. Clare Butler is also acknowledged for her careful review of English.

FUNDING

Open Access funding provided thanks to the CRUE-CSIC agreement with Springer Nature.

DECLARATIONS

The samples provider had no role in the design of the study; in the collection, analyses, or interpretation of data; in the writing of the manuscript; and in the decision to publish the results.

Conflict of Interest The authors declare no competing interests.

Open Access This article is licensed under a Creative Commons Attribution 4.0 International License, which permits use, sharing, adaptation, distribution and reproduction in any medium or format, as long as you give appropriate credit to the original author(s) and the source, provide a link to the Creative Commons licence, and indicate if changes were made. The images or other third party material in this article are included in the article's Creative Commons licence, unless indicated otherwise in a credit line to the material. If material is not included in the article's Creative Commons licence and your intended use is not permitted by statutory regulation or exceeds the permitted use, you will need to obtain permission directly from the copyright holder. To view a copy of this licence, visit <http://creativecommons.org/licenses/by/4.0/>.

REFERENCES

- Naik A, Kalia YN, Guy RH. Transdermal drug delivery: overcoming the skin's barrier function. *Pharm Sci Technology Today* [Internet]. 2000;3:318–26. Available from: <https://linkinghub.elsevier.com/retrieve/pii/S1461534700002959>
- Fahr A, Scherphof G. *Voigt's pharmaceutical technology*. Hoboken, NJ: Wiley; 2018.
- Latsch S, Selzer T, Fink L, Horstmann M, Kreuter J. Use of isothermal heat conduction microcalorimetry, X-ray diffraction, and optical microscopy for characterization of crystals grown in steroid combination-containing transdermal drug delivery systems. *Eur J Pharm Biopharm* [Internet]. *Eur J Pharm Biopharm*. 2004 [cited 2021 Nov 15];57:397–410. Available from: <https://pubmed-ncbi-nlm-nih.gov/sire.ub.edu/15019001>
- Santos P, Watkinson AC, Hadgraft J, Lane ME. Formulation issues associated with transdermal fentanyl delivery. *Int J Pharm* [Internet]. *Int J Pharm*. 2011 [cited 2021 Nov 15];416:155–9. Available from: <https://pubmed-ncbi-nlm-nihgov.sire.ub.edu/21723931>
- Sachdeva V, Bai Y, Kydonieus A, Banga AK. Formulation and optimization of desogestrel transdermal contraceptive patch using crystallization studies. *Int J Pharm*. Elsevier. 2013;441:9–18.
- Jenquin MR, McGinity JW. Characterization of acrylic resin matrix films and mechanisms of drug-polymer interactions. *Int J Pharm*. Elsevier. 1994;101:23–34.
- Drug-in-polymer solubility calculator for DURO-TAK adhesives. Available online. URL: <http://calculator.duro-tak.com/> (Accessed 20th November 2019)
- Tulloch IF. Pharmacologic profile of ropinirole: a non-ergoline dopamine agonist. *Neurology* [Internet]. Lippincott Williams and Wilkins. 1997;49. Available from: <https://pubmed.ncbi.nlm.nih.gov/9222275/-S62>.
- Drugbank database. Available online: <http://www.drugbank.com>. (Accessed 13 Jun 2018).
- Soler LI, Boix A, Lauroba J, Colom H, Domenech J. Transdermal delivery of alprazolam from a monolithic patch: Formulation based on in vitro characterization. *Drug Dev Ind Pharm* [Internet]. 2012;38:1171–8. Available from: <http://www.tandfonline.com/doi/full/10.3109/03639045.2011.643893>
- Jafri I, Shoaib MH, Yousuf RI, Ali FR. Effect of permeation enhancers on in vitro release and transdermal delivery of lamotrigine from Eudragit®RS100 polymer matrix-type drug in adhesive patches. *Prog Biomater*. 2019;8:91–100.
- International conference on harmonisation of technical requirements for registration of pharmaceuticals for human use”, Chapter “ICH Topic Q3C (R8) Impurities: Guideline for Residual Solvents
- Lentner MLC (ed.). *Geigy scientific tables*, 8th edition. Vol. 1. Units of Measurement. Body Fluids. Composition of the Body. Nutrition. 1981, 298 pp. Vol. 2. Introduction to Statistics. Statistical Tables. Mathematical Formulae. 1982, 241 pp. Vol. 3. *Physi. J Appl Toxicol* [Internet]. 1987; 7:413–413. Available from: <http://doi.wiley.com/10.1002/jat.2550070617>
- Shete Y, Pimpodkar N, Nalawade RS, Pore YV, Kuchekar BS. Spectrophotometric estimation of ropinirole hydrochloride in tablets. *Indian J Pharm Sci* [Internet]. Wolters Kluwer – Medknow Publications. 2009 [cited 2021 Jul 15];71 61–2. Available from: [/pmc/articles/PMC2810052](https://pubmed.ncbi.nlm.nih.gov/15019001)
- Zhang Y, Huo M, Zhou J, Zou A, Li W, Yao C, Xie S. DDSolver: an add-in program for modeling and comparison of drug dissolution profiles. *AAPS J* [Internet]. 2010;12:263–71. Available from: <http://link.springer.com/10.1208/s12248-010-9185-1>
- Costa P, Sousa Lobo JM. Evaluation of mathematical models describing drug release from estradiol transdermal systems. *Drug Dev Ind Pharm*. 2003;29:89–97.
- Paterna-Paterna J, Miñarro-Carmona M, Ticó-Grau JR, Boix-Montañés A. Release of ropinirole from acrylate-vinylacetate transdermal formulations: modulation based on polymer-drug interactions. *Proceedings*. 2020;78(1):38.
- Peppas NA, Sahlin JJ. A simple equation for the description of solute release. III. Coupling of diffusion and relaxation. *Int J Pharm*. 1989;57:169–72.
- Costa P, Sousa Lobo JM. Evaluation of mathematical models describing drug release from estradiol transdermal systems. *Drug Dev Ind Pharm* [Internet]. Taylor & Francis. 2003 [cited 2021 Jun 26];29:89–97. Available from: <https://www.tandfonline.com/doi/full/10.1081/DDC-120016687>
- Miravittles-Mille L. *Cristatografia Geometrica*. Barcelona: CEU ed; 1976. ISBN 84-7428-004-4
- Higuchi T. Rate of release of medicaments from ointment bases containing drugs in suspension. *J Pharm Sci* [Internet]. 1961;50:874–5. Available from: [https://jpharmsci.org/article/S0022-3549\(15\)33303-7/pdf](https://jpharmsci.org/article/S0022-3549(15)33303-7/pdf)
- DMSO Physical Properties | Gaylord Chemical [Internet]. [Accessed 2020 Dec]. Available from: <https://www.gaylordchemical.com/products/literature/physical-properties/>
- Ameen D, Michniak-Kohn B. Development and in vitro evaluation of pressure sensitive adhesive patch for the transdermal delivery of galantamine: effect of penetration enhancers and crystallization inhibition. *Eur J Pharm Biopharm*. 2019;139:262–71.
- Williams HD, Trevaskis NL, Charman SA, Shanker RM, Charman WN, Pouton CW, et al. Strategies to address low drug solubility in discovery and development. *Christopoulos A, editor. Pharmacol Rev* [Internet]. 2013;65:315 LP – 499. Available from: <http://pharmrev.aspetjournals.org/content/65/1/315.abstract>

Publisher's Note Springer Nature remains neutral with regard to jurisdictional claims in published maps and institutional affiliations.